

Excimer laser treatment of nickel-coated cast iron

C.N. Panagopoulos *, A.E. Markaki, P.E. Agathocleous

Laboratory of Physical Metallurgy, National Technical University of Athens, Zografos, 15780 Athens, Greece

Received 17 January 1997; received in revised form 11 April 1997

Abstract

Nickel-coated cast iron was laser treated using pulsed excimer radiation. The amount of processing was varied by varying the laser power density, number of pulses per step and the overlap between consecutive steps. Mixing of the coating and substrate elements was observed. The surface roughness was a non-linear function of the laser pulse number. Surface layers presented higher microhardness as compared with the untreated material. The corrosion resistance of the laser-treated material was found to be a function of the number of laser pulses. © 1998 Elsevier Science S.A.

Keywords: Excimer; Laser treatment; Surface alloying

1. Introduction

Recent research efforts have been concentrated on the development of surface layers with improved properties. An effective method of surface modification of a metal is laser alloying with a variety of alloying elements. The main characteristics of this process is the possibility of producing surface layers with a selection of alloy compositions tailor-made for the requirements. The use of high energy beams, such as laser beams, to induce local superficial modifications on the composition and microstructure of the near surface region of a metal has been the subject of several researchers.

There are three major types of lasers which are widely used by the scientific and industrial community. The use of cw CO₂ lasers is widespread for cutting, drilling, melting, welding, material removal, annealing and cladding applications. This is because of the high power levels that these lasers can emit. The major disadvantage of this laser is the very high light reflectivity at 10.6 μm which makes the absorption of the laser energy difficult. The pulsed Nd-YAG laser probably has a wider variety of applications than any other type of laser. The major application of this laser is in various forms of material processing: drilling, spot welding, and laser marking. Nd-YAG lasers emit lower energy levels compared with CO₂ lasers but their advantage is that

the reflectivity is lower at 1.06 μm. Pulsed excimer lasers are now beginning to make their presence known. They are used primarily for materials processing, medical applications, photolithography, and pumping of dye lasers. In the materials processing area, excimer lasers are advantageous because of their wavelength and energy per pulse. The absorption coefficient for most materials is much greater for ultraviolet wavelengths than for infrared wavelengths (CO₂ and Nd-YAG lasers). Moreover it is possible to supply high energy densities in a very short period of time (order of ns). The disadvantage of this laser is the lower energy levels that are emitted compared with the other two types of lasers [1,2]. The fact that a lot of research has been concentrated on infrared processing combined with the presence of a relatively new laser like excimer laser, makes the processing in UV an attraction for research.

The most recent applications of the excimer laser in the technological field of surface metallurgy are described below.

Hirvonen et al. [3] have implanted Ti ions into Fe surfaces forming a thin amorphous surface alloy by excimer laser irradiation. This alloy improves the wear and friction properties of the surface as compared with the unimplanted surface.

Jervis et al. [4] used excimer laser radiation to mix thin layers of Ti into AISI stainless steel. Different numbers of shots at a fluence about twice the threshold for melting varied the amount of mixing. When mixing

* Corresponding author.

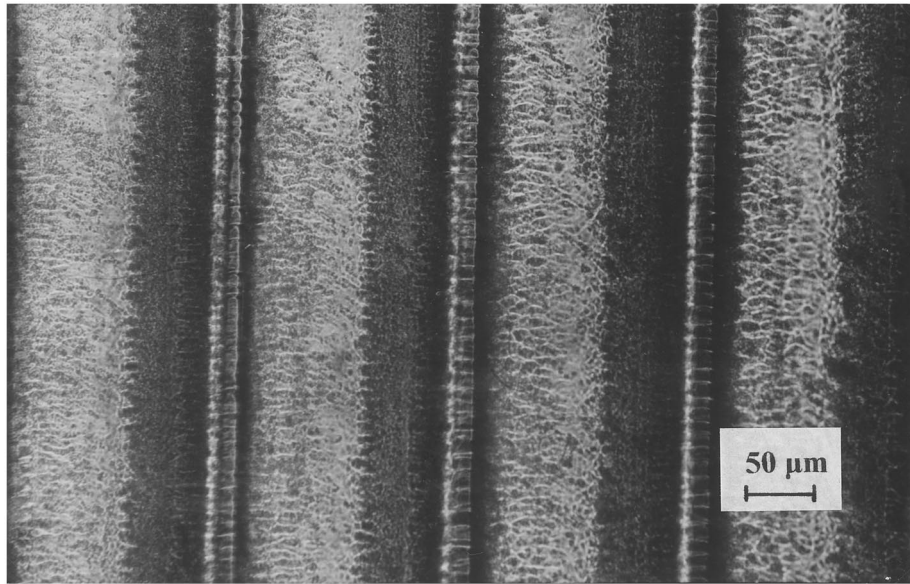


Fig. 1. Micrograph of the surface of nickel-coated cast iron after laser treatment (250 MW cm^{-2} power density, 25 pulses per step, 30% overlapping).

is sufficiently complete, an amorphous surface layer is formed with Ti substituting for Fe on a one-to-one basis in the alloy.

Michaelides and Panagopoulos [5] examined electrodeposited zinc on a copper substrate irradiated with an excimer laser. Zinc atoms were found to diffuse into the copper substrate. The surface morphology and structure after the laser treatment were examined.

Excimer laser treatment was performed on a copper surface [6]. The magnitude of the residual stress on the copper-surface layers changed from tensile to compressive after the laser treatment.

Panagopoulos et al. [7] irradiated electroplated zinc on an aluminium substrate with a high power excimer laser. Zinc atoms were found to diffuse into the substrate. The surface microstructure after the laser treatment was mainly dendritic. The surface roughness was a function of the lasing conditions.

Surface laser treatment with an excimer laser KrF on a titanium surface was described by Badekas et al. [8].

Panagopoulos et al. [9] irradiated electrodeposited copper on a mild steel substrate, which was first coated by a nickel strike. Laser-induced surface structures were observed. By using a simple formula, they estimated the threshold value of power density causing the surface layers of copper to melt. EDX analysis showed that nickel and iron atoms diffuse into the copper coating. Microhardness measurements and X-ray diffraction were also performed.

It is often desirable to impart certain properties of one relatively expensive material to a less expensive substrate by applying a thin coating of the former to the latter. In particular, in this study, a nickel coating

was electrodeposited on a cast iron substrate prior to laser treatment.

2. Experimental procedure

The substrate material was a low alloying pearlitic cast iron with a chemical composition of 3.45 wt.% carbon, 2.39 wt.% silicon, 0.78 wt.% manganese, 0.29 wt.% phosphorus, 0.20 wt.% copper, 0.12 wt.% sulphur, 0.13 wt.% chromium, (0.07 wt.% nickel). Specimens with dimensions of $3.0 \times 1.0 \text{ cm}^2$ and thickness 1.2 mm were used in this study.

The specimens were annealed at 400°C for about 1 h, to eliminate machining residual stresses. The method used before electrodeposition to ensure cleanliness of the surface and to improve the adhesion was; alkaline cleaning (0.2 M NaOH solution at 70°C for 20 min) and acid pickling (HCl acid) with inhibitor.

Nickel electrodeposition took place in a Watts type bath. The composition of the bath and the operating conditions were: $\text{NiSO}_4 \cdot 6\text{H}_2\text{O}$, 317 g l^{-1} ; $\text{NiCl}_2 \cdot 6\text{H}_2\text{O}$, 45 g l^{-1} ; H_3BO_3 , 37 g l^{-1} (pH 3–3.5, $T = 57 - 60^\circ\text{C}$).

The current density was kept constant at 4 A dm^{-2} . One thickness of nickel coating has been chosen: 15 μm .

After the nickel deposition, a Lambda Physik excimer laser, operating at a wavelength of 248 nm with a pulse length of 25 ns, using a KrF gas mixture, was used to treat the surface of the nickel-coated cast iron specimens. The laser beam pulse had a Lorentzian shape. Processing was done in ambient air with no shield gas. The area of the incident laser beam was

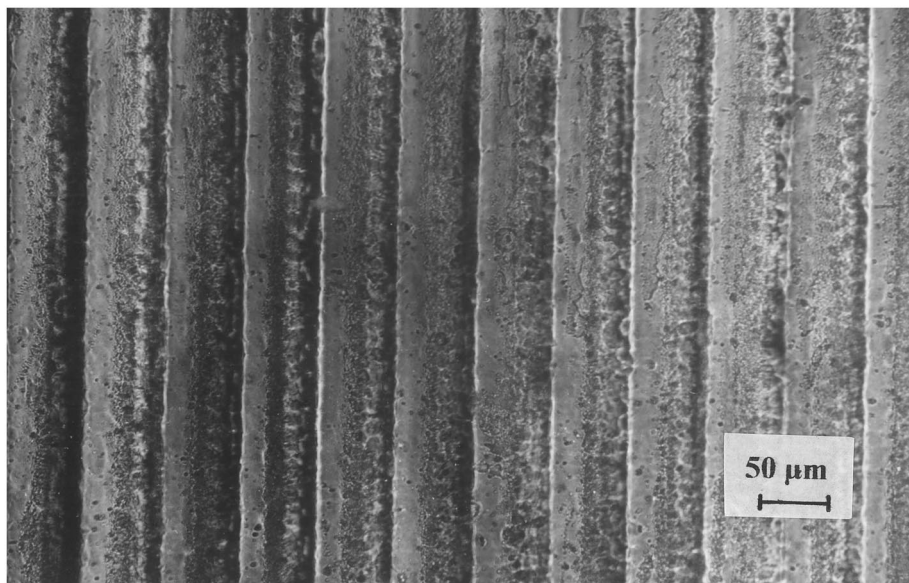


Fig. 2. Micrograph of the surface of nickel-coated cast iron after laser treatment (200 MW cm^{-2} power density, 50 pulses per step, 80% overlapping).

$1.0 \times 1.0 \text{ cm}^2$. Each specimen was irradiated under different conditions. The variables of the irradiation were: the power density and the number of pulses per step. In order to observe the influence of each laser parameter, all the experiments were carried out in such a way that one parameter was kept constant while the other varied. The power density varied between 120 and 325 MW cm^{-2} and the pulses per step varied between 25 and 400 pps. The steps were overlapped 30 and 80%, the pulse frequency was 30 Hz and the surface was given a single scan.

After the laser treatment, surface morphology and cross-sections of the nickel-coated cast iron samples were examined by means of optical microscopy (Zeiss microscope). The latter were mechanically polished with a series of SiC abrasive papers (No. 220, 400, 600, 800, 1000, 1200) and afterwards polished to $1 \mu\text{m}$ with diamond paste.

Laser-treated specimens were introduced into a scanning electron microscope (Jeol-6300) equipped with an energy dispersion X-ray spectrometer (EDX) to determine the elemental concentration.

The laser-treated specimens were examined by using a Siemens diffractometer with Cu K_α radiation ($\lambda = 0.15405 \text{ nm}$).

A profilometer (Mahr Perthen) was used to measure the roughness of the laser-treated surfaces by moving its stylus parallel to the laser steps. The parameter measured for this purpose was the arithmetic mean deviation of the roughness profile R_a . The stylus was moved a distance of 4 mm to measure. For any particular surface, R_a was measured across ten different profiles and the mean was taken to be the representa-

tive value. The standard deviation of each set of results was calculated.

Microhardness measurements were made on polished cross-sections of laser-treated and untreated samples, with a Vickers indenter of a microhardness tester. A load of 6.2 g and loading time 15 s were selected for measuring the microhardness. Each hardness value was the average of seven measurements and the standard deviation of each set of results was also calculated.

The corrosion resistance of both laser- and non-laser-treated samples was evaluated using a 0.5 M NaCl aqueous solution (pH 5.1) of 290 K temperature for a period of 3 days. For corrosion testing the samples were embedded in a resin, leaving an exposed area of about $1.0 \times 1.0 \text{ cm}^2$ for investigation. The reference electrode was a saturated calomel electrode (SCE).

3. Experimental results and discussion

Bright field micrographs in Figs. 1 and 2 show the surface morphology after performing successive steps overlapped 30 and 80%, respectively. The distance between successive steps is clearly observed in pulsed-laser treated specimens. Overlapping successive steps induces a thermal experience in the neighbouring steps so that there is some back tempering. The surface is characterized by a change in brightness, which implies that the surface is no longer flat. Anthony and Cline [10] examined how surface-tension gradients generated by temperature gradients can cause significant rippling of a laser-melted surface.

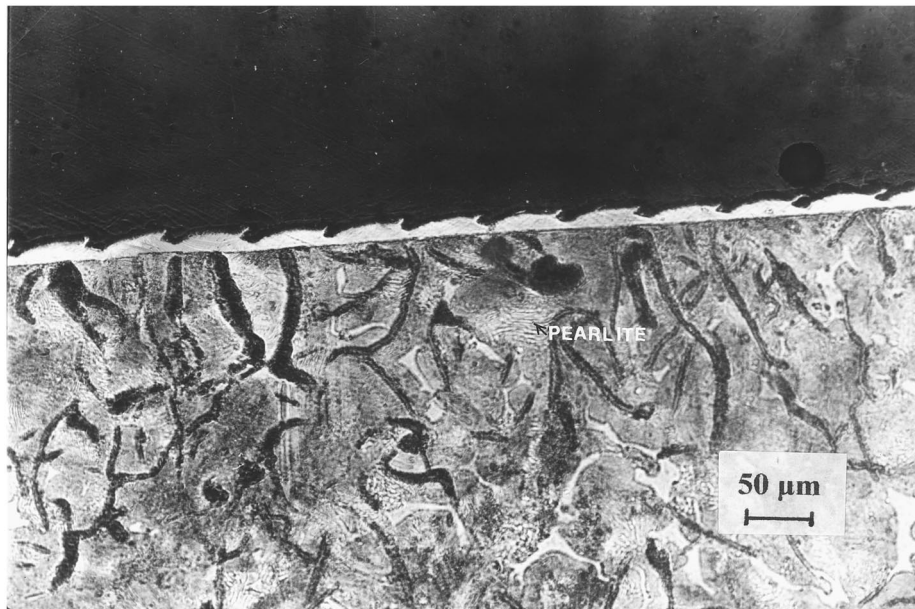


Fig. 3. Cross-section of a nickel-coated cast iron specimen after laser irradiation (200 MW cm^{-2} power density, 200 pulses per step, 80% overlapping).

A typical micrographic observation (Fig. 3) on a cross-section (etched in 2% nital to reveal microstructure of cast iron) reveals the existence of: (a) substrate—a cast iron structure is observed with two components, pearlite and lamellar graphite. The microhardness of pearlite (load 15.8 g) was observed in the range 240–270 HV. (b) nickel coating; highly distorted macrostructure resulting from the laser treatment [10].

After laser treatment, X-ray diffraction spectra revealed the formation of surface NiO film (Fig. 4). The formation of oxides may well be due to strong surface melt–environmental interactions. It should be noted that the experiments were performed in ambient air and not in a shielded gas atmosphere.

Fig. 5 shows the surface roughness R_a of laser treated specimens as a function of the number of pulses per step. Increasing the number of pulses per step, i.e. longer interaction time leads to an increase of laser energy absorption by the nickel surface. Thus there is an increase in the surface roughness.

As the laser beam moves over the specimen surface, the temperature rises and thermal energy is transferred into the specimen. After performing the EDX analysis it was observed that iron atoms from the cast iron substrate were detected into the nickel coating. Also, nickel atoms were found in the cast iron substrate. Due to the iron mixing with nickel and vice versa, a surface alloy was formed in the nickel coating and at the top layers of cast iron substrate. The iron and nickel concentration (at.%) as a function of depth for different lasing conditions were shown in Figs. 6–9 respectively.

Increasing each of the lasing parameter greater concentration of iron and nickel atoms at the nickel coating and the cast iron substrate respectively were observed. In particular, increasing the laser power density, more heat is deposited at the surface and transferred into the internal layers of the specimen. This leads to an increase of temperature that causes an increase in the number of mixed atoms, i.e. the thickness of surface alloy (Figs. 6 and 8). The effect of increasing the number of pulses per step is similar to the effect of increasing the laser power density; when a high number of pulses is used, the interaction time is long; this means that more energy is transferred into the specimen and therefore greater mixing between nickel and iron atoms was noted (Figs. 7 and 9).

Fig. 10 shows the effect of laser power density on the average microhardness of nickel. Increasing laser power density leads to an increase in nickel microhardness. EDX analysis showed that mixing became more intense as this lasing parameter increased. Examining the Fe–Ni phase [11] diagram the following observations can be made. For low iron content we have a substitutional solid solution for iron atoms in FCC nickel, phase γ (Hume Rothery's rules which control the tendency for the formation of substitutional solid solutions are satisfied). For higher iron content, the phase diagram shows that at equilibrium there are two phases α and γ , field ($\alpha + \gamma$) (α phase is a substitutional solid solution for nickel atoms in α -Fe crystal structure).

The formation of solid solutions between iron and nickel causes the increase in nickel microhardness. Solid solutions are harder and stronger than pure metals [12].

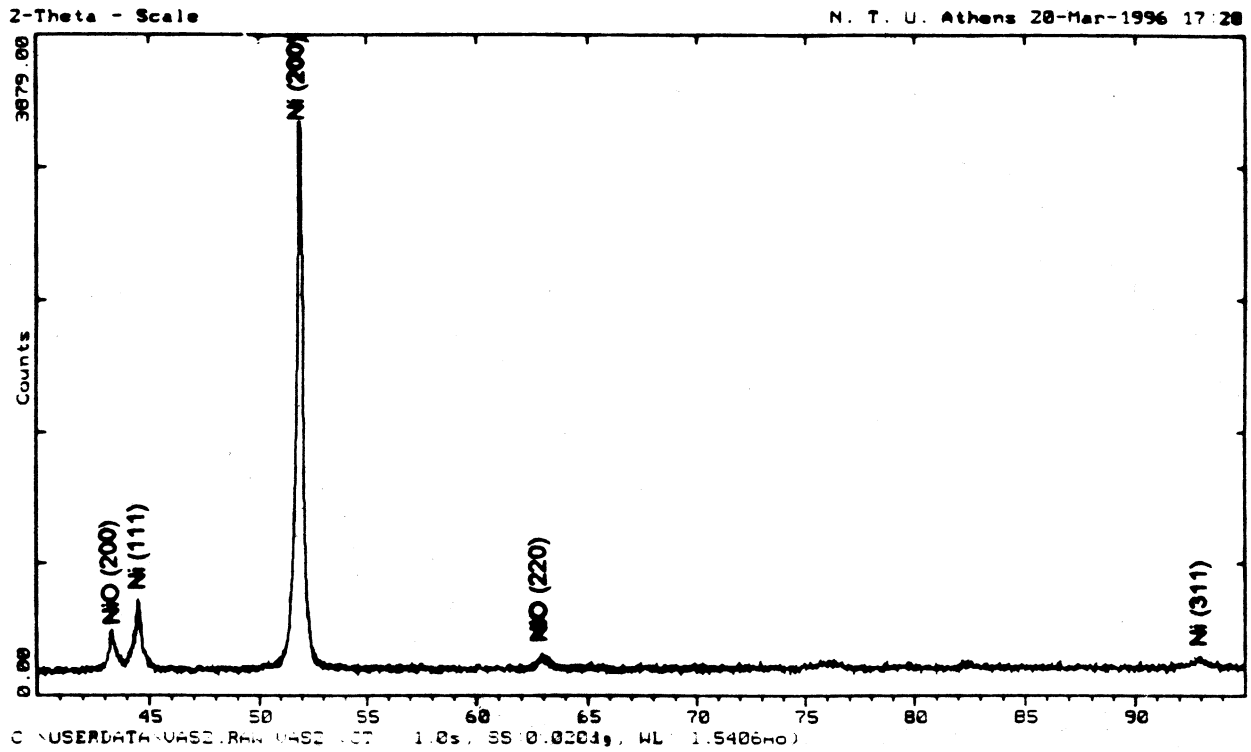


Fig. 4. X-ray diffractometry data from laser-treated surface (lasing conditions: 325 MW cm⁻² power density, 200 pulses per step, 80% overlapping).

As the iron concentration in the nickel coating increases the strengthening becomes more intense. In order to show the improvement in mechanical properties, microhardness measurements have been performed on the untreated nickel coating and were in the range 190–200 HV.

Fig. 11 shows the corrosion potential versus time.

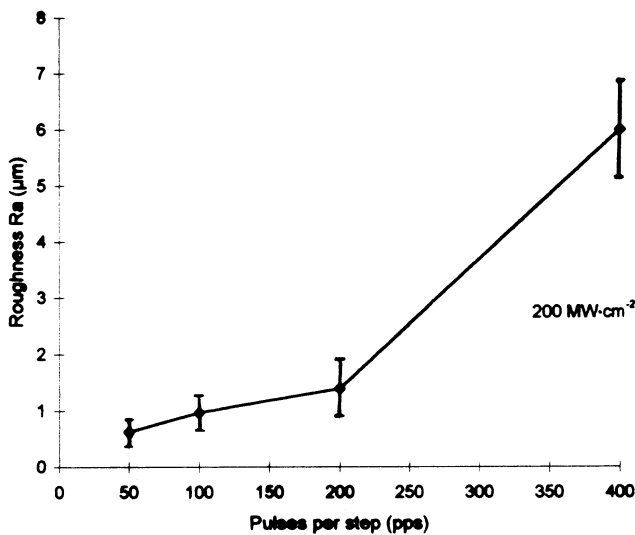


Fig. 5. Surface roughness of laser-treated specimens as a function of the number of pulses per step.

The untreated sample has the noblest potential (more positive) compared with the laser-treated specimens. The corrosion potential of the untreated specimen tends to decrease slightly with increasing time. The corrosion potential of the sample irradiated by 100 pulses per step decreases with increasing time. Finally the corrosion potential of a specimen after irradiation by 400 pulses

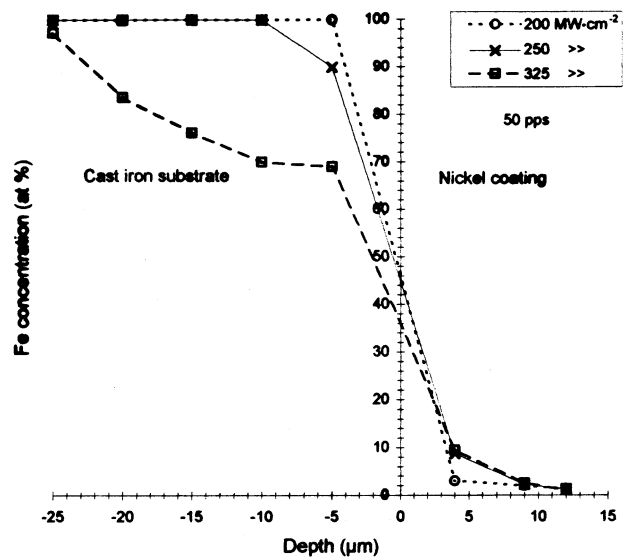


Fig. 6. Iron concentration (at.%) as a function of depth (EDX analysis).

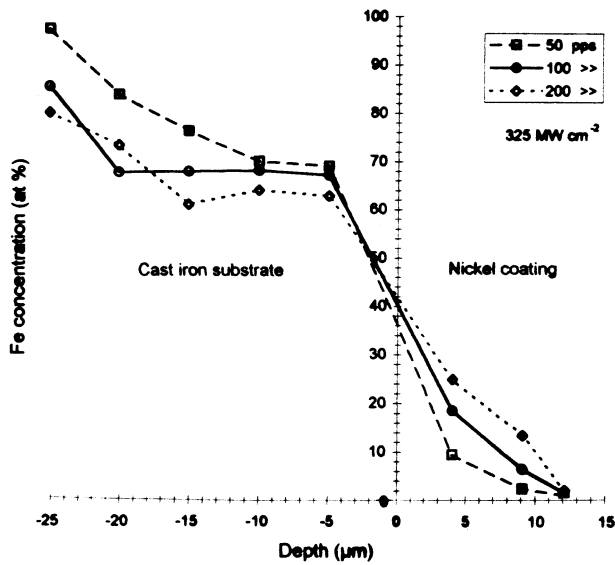


Fig. 7. Iron concentration (at.%) as a function of depth (EDX analysis).

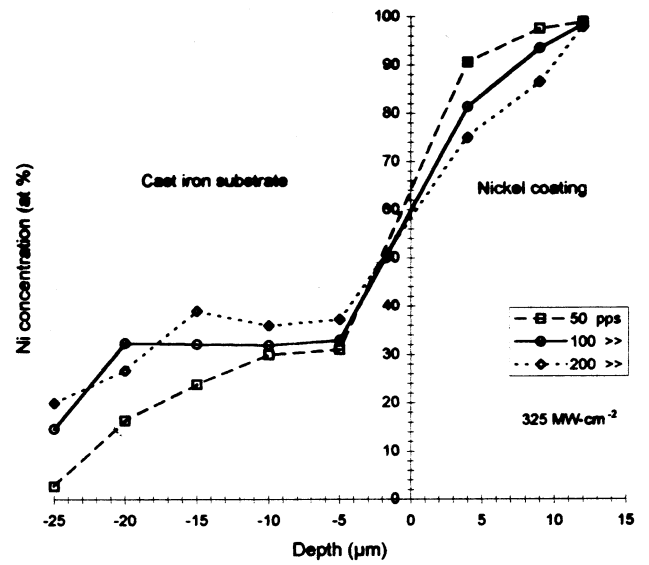


Fig. 9. Nickel concentration (at.%) as a function of depth (EDX analysis).

per step decreases with increasing time up to the first 60 min and then remains approximately constant all through the test.

The laser-treated specimens exhibit lower corrosion-resistance compared with the untreated specimen. This might be attributed to the following reason: as mentioned above, laser treatment creates significant rippling and roughening of the treated surface. The ripple structure, forming higher energy areas, causes the nucleation of pits (localized corrosion). Pitting corrosion is caused by the chloride ions as they form a free acid (H^+Cl^-) of high strength. The generation of this acid stimulates the dissolution of most metals, including nickel [13].

For the laser-treated specimens, it is observed that as the number of pulses per step increases, the corrosion potential becomes more negative. This observation combined with the surface roughness measurements (Fig. 5) can be attributed to the effect of higher surface roughness leading to the higher corrosion of the specimens.

4. Conclusions

Irradiation of nickel-coated cast iron surface by a

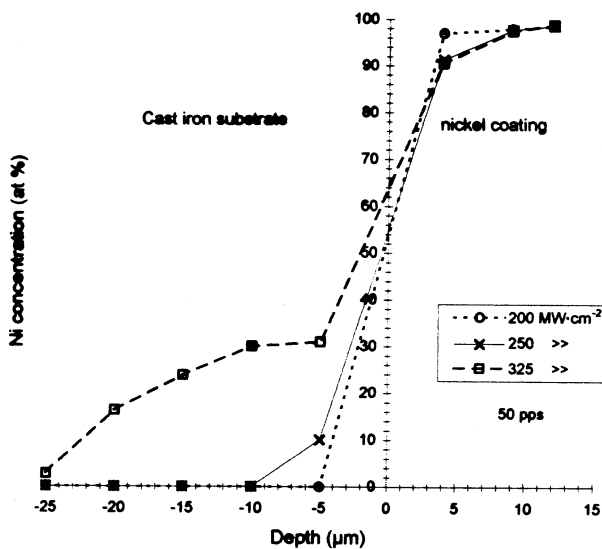


Fig. 8. Nickel concentration (at.%) as a function of depth (EDX analysis).

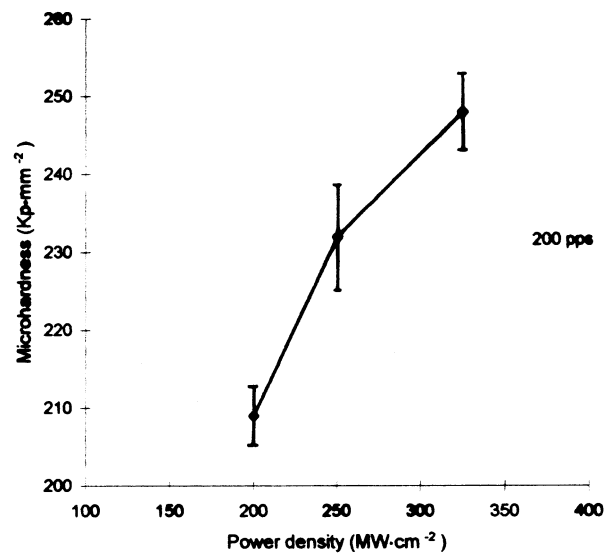


Fig. 10. Effect of laser power density on the average microhardness of nickel.

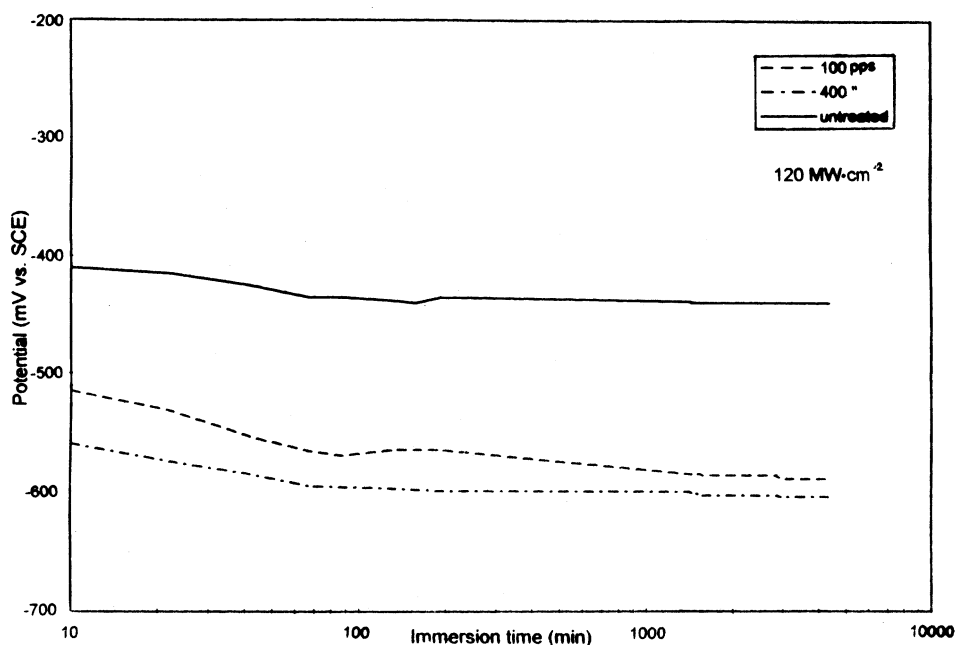


Fig. 11. Corrosion potential vs. immersion time.

high intensity excimer laser yielded the following results:

(1) After the laser treatment a roughened surface was observed. The roughness of the surface was found to be dependent on the number of laser pulses.

(2) Iron atoms from the cast iron substrate were observed into the nickel coating. Also, nickel atoms were found in the substrate.

(3) Solid solutions formed between iron and nickel caused the increase in nickel microhardness.

(4) The corrosion behaviour of the laser-treated specimens was found to be a function of the number of laser pulses.

Acknowledgements

The authors wish to thank Dr J. Inglessis (Hellenic Force) for performing the EDX analysis of laser-treated specimens and Professor K. Fotakis (University of Crete) for providing laser facilities.

References

- [1] J. Jervis, P. Hirvonen, M. Nastasi, *Lubric. Eng.* 48 (1991) 141–146.
- [2] W.T. Silfvast, *Laser Fundamentals*, Cambridge University Press, 1996, pp. 420–455.
- [3] P. Hirvonen, J.W. Mayer, M. Nastasi, D. Stone, *Nucleic Instrum. Methods B23* (1987) 487.
- [4] T.R. Jervis, M. Nastasi, T.G. Zocco, J.A. Martin, *Appl. Phys. Lett.* 53 (1988) 75.
- [5] A. Michaelidis, C.N. Panagopoulos, *Proc. 9th Greek Confer. on Lasers*, Greek Electrooptical Soc., Athens, 1992, p. 250.
- [6] C. Panagopoulos, A. Michaelidis, *J. Mater. Sci.* 27 (1992) 1280.
- [7] C.N. Panagopoulos, G. Christou, G. Daurelio, *Trans. Inst. Metal Finish.* 71 (1993) 65.
- [8] H. Badekas, C. Panagopoulos, S. Economou, *J. Mater. Process. Technol.* 44 (1994) 54.
- [9] C.N. Panagopoulos, A. Markaki, E. Honzopoulos, *J. Mater. Sci.* 32 (1997) 1425.
- [10] T.R. Anthony, H.E. Cline, *J. Appl. Phys.* 48 (1977) 3888.
- [11] M. Hansen, *Metallurgy and Metallurgical Series, Constitution of Binary Alloys*, 2nd ed., McGraw-Hill, New York, 1958, pp. 677–682.
- [12] G.E. Dieter, *Mechanical Metallurgy*, SI Metric edn., McGraw-Hill, London, 1988, pp. 203–207.
- [13] M.G. Fontana, *Corrosion Engineering*, 3rd edn., McGraw-Hill, New York, 1986, pp. 66, 69.